STRUCTURE AND DYNAMICS OF MEMBRANOUS INTERFACES

Edited by

Kaushik Nag

Memorial University
St. Jhon's, Newfoundland and Labrador
Canada

A John Wiley & Sons, Inc., Publication

STRUCTURE AND DYNAMICS OF MEMBRANOUS INTERFACES

Edited by

Kaushik Nag

Memorial University
St. Jhon's, Newfoundland and Labrador
Canada

A John Wiley & Sons, Inc., Publication

CHAPTER 12

Thermodynamics of the Nervous Impulse

THOMAS HEIMBURG and ANDREW D. JACKSON

Niels Bohr Institute, University of Copenhagen, Copenhagen, Denmark

CONTENTS

Structure and Dynamics of Membranous Interfaces, edited by Kaushik Nag

12.1 INTRODUCTION

12.1.1 Propagation of Pulses Along Nerve Membranes

Since the classical paper of Hodgkin and Huxley [1], nerve pulses have been explained as voltage pulses generated by the transient opening of ion channel proteins, and the resulting flux of ions across the nerve membrane. Even though this picture is popular and described in numerous textbooks, there exists quite compelling evidence that it cannot be correct. Several authors have found reversible temperature changes and reversible heat release during the action potential of both myelinated and nonmyelinated nerves. This finding indicates that the underlying basis of nerve pulse transmission must be reversible physics while the Hodgkin–Huxley model is exclusively based on irreversible phenomena. Furthermore, various changes in mechanical properties and changes in membrane state have been observed. We introduce here the thermodynamics of nerves and biological membranes. We show that the physiological conditions imply the possibility of localized density pulse propagation along the nerve membrane that is in agreement with the thermodynamics findings in nerves.

12.1.2 Thermodynamics of Biological Systems

Thermodynamics is one of the foundations of physics. It is based on two fundamental postulates: the conservation of energy and the maximum entropy principle. Thermodynamics is strictly true on all scales of physics from atomic scales to cosmology. Thus thermodynamics is also the theory underlying biological processes.

The first law assumes the form

$$dE = T\,dS - p\,dV - \Pi\,dA - f\,dl + \psi\,dq + \cdots + \sum_i \mu_i\,dn_i \tag{12.1}$$

Each term on the right-hand side is the product of an intensive variable (independent of system size) and the differential of an extensive variable (dependent on system size). The second law can be expressed as

$$dS = dS_r + dS_i \tag{12.2}$$

where S is the entropy. S_r is the reversible part of the entropy related to the reversible adsorption or release of heat given by

$$dS_r = \frac{dQ}{T} \tag{12.3}$$

The irreversible part S_i is related to spontaneous changes within the system that are not coupled to heat exchange with the environment and the performance of work on the exterior. This part is always larger than zero:

$$dS_i \geq 0 \tag{12.4}$$

The irreversible part of the entropy is typically responsible for the progress of chemical reactions and other equilibration processes.

The laws of thermodynamics also hold when the system under consideration is not in equilibrium. The second law states that each system approaches the state of maximum entropy, that is, the most probably state. Around this state one finds fluctuations due to thermal motion. In the field of nonequilibrium thermodynamics it is typically assumed that on small scales detailed balance (i.e., microscopic reversibility) is obeyed. Thus, nonequilibrated systems also rely on the laws of equilibrium thermodynamics.

The maximum entropy law applies to the complete system under consideration but not to arbitrarily chosen subsystems. One can easily construct examples where the second law holds for the total system but not for individual parts. For instance, two gas containers with different pressure that are coupled by a piston are not in equilibrium (Fig. 12.1). After equilibration, the pressure in both containers is the same. (In fact, in each equilibrated system the intensive quantities T, p, Π, ψ, μ_i ... are homogeneous.) During the equilibration process, the volume of one container increases and the volume of the other one decreases. Thus the entropy of one container increases while that of the other container decreases. The total entropy, however, approaches a maximum. Another example would be the cold unfolding of proteins. It is well known that proteins denature (or unfold) upon temperature increase. During this process the configurational entropy of the protein backbone increases. Many proteins, however, also denature upon cooling to temperatures far below room temperature [2]. This is an unexpected (and not very well-known) phenomenon that is related to the strong temperature dependence of the interactions of proteins with water. During cold unfolding, the entropy of the amino acid chains increases upon cooling. The laws of thermodynamics state, however, that entropy always decreases with decreasing temperature. How then is cold unfolding possible? In fact, cold unfolding does not violate the laws of thermodynamics because the entropy of the proteins including the entropy of the associated water shell decreases upon cold unfolding even though the entropy of

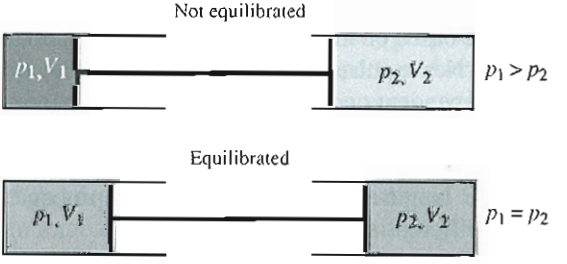

Figure 12.1 Two gas containers with different pressures that are coupled by a piston. After equilibration, the pressure in both containers is the same. The entropy of the total system has increased. The entropy of the right-hand gas container, however, has decreased. Thus the maximum entropy law does not hold for arbitrary subsystems if they are coupled to other systems.

the chains alone increases. The entropy increase of the chains is compensated by the decrease in the entropy of the water associated to the protein. We learn from this that the laws of thermodynamics apply to the whole system but not to subsystems. This statement is especially important when considering biological systems. Much of the research on biological systems focuses on individual molecules and their function. The proteins are considered separately from the membrane lipids. Typically, experiments on these molecules are done in test tubes at large dilution, where the molecule under consideration may be considered individually. It would, however, be a mistake to assume that one can understand the behavior of biological organisms by adding the functions of the individual molecules. In the biological environment molecules may act in a cooperative manner. The thermodynamic laws apply to the cell as a whole rather than to the isolated individual molecules. Thus the understanding of individual molecules may not necessarily lead to an understanding of complex biological systems.

If a system is not in equilibrium, the thermodynamic forces drive the system back to equilibrium. The progress of chemical reactions, diffusion processes, electrical currents, and soon are consequences of these forces. Typically, the thermodynamic forces consist in the gradients of the intensive quantities, for example, $-\text{grad}\, T$, $-\text{grad}\, \psi$, and $-\text{grad}\, \mu_i$. An exception is chemical reactions of nature $\nu_A \cdot A + \nu_B \cdot B + \cdots \longleftrightarrow \nu_C \cdot C + \nu_D \cdot D + \cdots$ (with the stoichiometries ν_i), where the thermodynamic force is given by the affinity A of a reaction defined by $A = -\sum \nu_i \mu_i$. Thermodynamic forces determine the progress of all reactions. All molecular species enter the thermodynamic equations via their chemical potentials. Thus thermodynamics is also applicable to nonequilibrium systems.

12.1.3 Macroscopic Versus Microscopic Models in Biology

Considering biological membranes, the previous statements on the entropy of large systems imply that the laws of thermodynamics apply to the membrane as a whole but not necessarily to each isolated molecule in this membrane when they interact with other molecules. Therefore it is dangerous to base theories of large systems on the behavior of single molecules.

In this chapter we discuss the propagation of nerve pulses. The textbook pictures for these phenomena are based on the action of single molecules and, in particular, on ion channel proteins. Nerve pulse propagation has commonly been explained by the voltage- and time-dependent opening and closing of such ion channels.

Models based on microscopic detail contain some further risks. A well-accepted strategy in physics is to search explanations of phenomena by using models of similar length scale. For instance, the propagation of sound is well described by the differential equation

$$\frac{\partial^2 \rho}{\partial t^2} = c_0^2 \frac{\partial^2 \rho}{\partial x^2} \tag{12.5}$$

where c_0 is the speed of sound and ρ is the density. It is a function of the isentropic compressibility, κ_S, and is given by $c_0 = \sqrt{1/\kappa_S \rho}$. This equation holds

for all gases independent of their molecular composition. It would be impossible to understand the propagation of sound on the basis of molecular mechanisms, for example, by applying molecular dynamics simulations. This is because sound propagation is basically an entropic phenomenon involving ensemble properties on large scales, that is, on the order of their wavelength. It is therefore more meaningful to determine the compressibility on a macroscopic scale.

A similar case is the propagation of the nerve pulse in its presently accepted picture. Hodgkin and Huxley proposed a model in 1952 in which they explained the features of a nerve pulse on the basis of individual ion channel proteins that open and close in a voltage- and time-dependent manner [1]. The typical diameter of an ion channel is about 5 nm. The nerve pulse in a myelinated nerve propagates at about 100 m/s and lasts about 1 ms, resulting in a typical pulse length of about 10 cm. A nonmyelinated squid axon displays a velocity of about 25 m/s and a length of 3 ms, corresponding to 6 cm. Thus the length scale of the nerve pulse is about 2.5×10^7 times larger than that of the ion channels. This is a similar difference in scale as, for instance, a coffee cup and the size of Europe. Nobody, however, would tend to explain macroscopic phenomena of the length scale of Europe (e.g., earthquakes, growth of mountain chains, or large storms) on the basis of objects the size of a coffee cup. Similar differences in scale, however, form the basis for the biological models of nerve pulses.

In this chapter we wish to apply the above concepts to the propagation of nerve pulses. During nerve pulses, in phase with voltage changes, one finds a reversible release of heat. We outline next that this implies that the nervous impulse is a consequence of reversible physics. To be able to describe the underlying thermodynamic theory, we describe in the next section the basics of the textbook model for nerve pulses, in particular, the Hodgkin–Huxley model that explains the propagating pulse as a consequence of specific resistors called ion channels. We show that this model predicts changes in heat release that are inconsistent with experimental findings.

12.1.4 The Hodgkin–Huxley Model

Nerve cells possess extended axons along which voltage pulses called "action potentials" can propagate. In 1952, Hodgkin and Huxley proposed a model for the action potential that was based on the conductance properties of nerve membranes obtained by voltage clamp experiments [1]. In such experiments an electrode is inserted into a nerve, and a voltage difference between the inside and outside of the nerve is applied. Since the voltage is kept constant along the whole nerve, no pulses propagate in such experiments. Schematically, this experiment is shown in Fig. 12.2.

The transmembrane current is described by

$$I_{\mathrm{m}} = C_{\mathrm{m}} \frac{dU}{dt} + g_{\mathrm{K}}(U - E_{\mathrm{K}}) + g_{\mathrm{Na}}(U - E_{\mathrm{Na}}) + g_{\mathrm{L}}(U - E_{\mathrm{L}}) \qquad (12.6)$$

where $g_{\mathrm{K}}(V, t)$ and $g_{\mathrm{Na}}(V, t)$ are voltage- and time-dependent conductivities of potassium and sodium channels, and E_{K} and E_{Na} are the corresponding Nernst

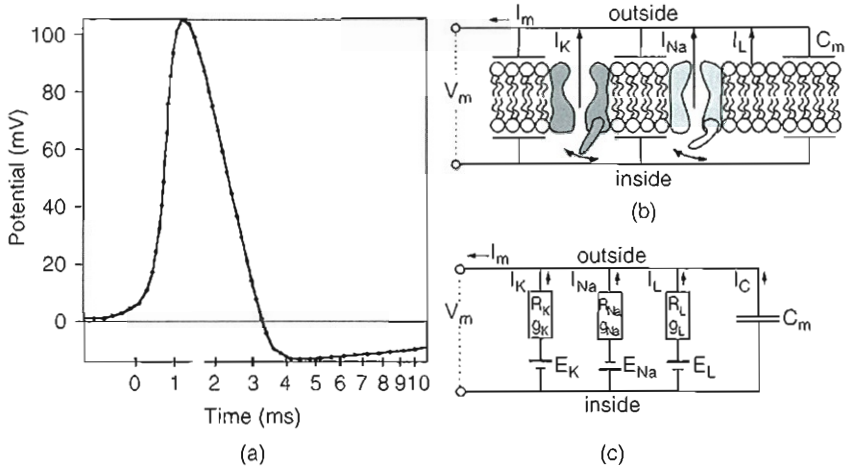

Figure 12.2 Molecular basis of the Hodgkin–Huxley model. (a) The action potential as given by Hodgkin and Huxley [1]. (b) Schematic drawing of the membrane including sodium and potassium channel proteins that are selective conductors for sodium and potassium. (c) Equivalent circuit picture of the same membrane (from Ref. 3).

potentials that depend on the ion concentration differences inside and outside the nerve cell. For the squid axon they are $E_K = -80$ mV and $E_{Na} = +60$ mV. The terms with index L correspond to leakage currents of other ions and will not be considered in the following. Typical maximum conductances of squid axon membranes are on the order of 4×10^{-3} S/cm^2 (=A/V·cm^2) for both potassium and sodium channels. The capacitance of the membrane is on the order of 1 μF/cm^2 (which is calculated for a capacitor of capacitance $C_m = \varepsilon \cdot \varepsilon_0 \cdot A/d$ with plate separation of $d = 3.5$ nm (thickness of the hydrophobic core of the membrane) and a dielectric constant within the membrane of $\varepsilon = 4$).

Equation (12.6) contains currents through resistors and capacitive currents. The charge on a capacitor is given by $q = C_m U$. Thus the capacitive current is given by

$$I_C = \frac{dq}{dt} = C_m \frac{dU}{dt} + U \frac{dC_m}{dt} \tag{12.7}$$

Thus in the Hodgkin–Huxley description, it was assumed that the capacitance stays constant. We show later that this is probably incorrect. Note also that the neglected term dC_m/dt has the units of a conductance [38].

The differential equation for the propagation of the nerve pulse is

$$\frac{a}{2R_i} \frac{\partial^2 U}{dt^2} = C_m \frac{\partial U}{dt} + g_K(U - E_K) + g_{Na}(U - E_{Na}) \tag{12.8}$$

where a is the radius of the nerve and R_i is the internal resistance of the aqueous medium along the nerve interior. According to Hodgkin and Huxley [1], the maximum amplitude of the potassium current is on the order of 800 $\mu A/cm^2$, while the maximum sodium current amplitude is about $+800\ \mu A/cm^2$.

The Hodgkin–Huxley model relies on equivalent circuits (Kirchhoff circles). Since the model contains resistors one expects a heat production described as

$$\frac{dQ}{dt} = P = U \cdot I \cong \sum_i g_i (U - E_i)^2 \tag{12.9}$$

In the following we want to estimate the heat observed by a heat sensor placed (e.g., a thermocouple) on the nerve surface.

Using Eq. (12.9), one obtains a heat production for the potassium channels at maximum voltage of about

$$\frac{dQ}{dt} \approx 4 \times 10^{-3} \frac{\mathrm{A}}{\mathrm{V} \cdot \mathrm{cm}^2} \cdot (0.1\mathrm{V})^2 = 40 \times 10^{-6} \frac{\mathrm{J}}{\mathrm{s} \cdot \mathrm{cm}^2} \tag{12.10}$$

This is the heat per cm^2 of heat sensor surface released per second. The heat produced by the sodium currents should be of similar order. The data underlying this calculation have been taken from the original paper of Hodgkin and Huxley [1] on the squid axon. Since heat release is independent of the direction of the current, heat release should always be positive.

The energy of the membrane capacitor at maximum voltage is

$$E_C = \frac{1}{2} C U^2 = \frac{1}{2} \times 10^{-6} \frac{\mathrm{F}}{\mathrm{cm}^2} \cdot (0.1\mathrm{V})^2 = 5 \times 10^{-9} \frac{\mathrm{J}}{\mathrm{cm}^2} \tag{12.11}$$

This corresponds to the heat recorded by 1 cm^2 of heat sensor if the membrane is charged from 0 to 100 mV. Simultaneously, this is the energy of the nerve pulse per unit area.

The squid axon has a propagation velocity of about 25 m/s, and the action potential lasts about 3 ms when measured at one point on the nerve. This results in a pulse length of about 6–9 cm, which is quite extended.

This means that the heat dissipated during the squid action potential by Na^+ and K^+ currents (that would be measured at one point of the nerve) is on the order of (cf. Eq. (12.10))

$$Q = 200 \times 10^{-9}\ \mathrm{J/cm}^2 \tag{12.12}$$

The heat from the currents that would be recorded by a heat sensor is therefore more than one order of magnitude larger than the energy necessary to charge the capacitor. The latter is the energy of the action potential, because the information transported during the action potential lies in the propagating segment of charged capacitor. Most of the chemical free energy stored in the ion concentration gradients is therefore dissipated. Assuming a membrane density of about 1 g/cm^3

and a membrane thickness of 5 nm, one obtains a heat of about 0.4 J/g from the ion currents of membrane while the energy of the pulse as calculated from the capacitive energy is on the order of 0.01 J/g of membrane. All these calculations are estimates intended to indicate the order of magnitude of the respective effects.

The action potential is a dissipative process due to the flux of ions through resistors from the high concentration to the low concentration side. Thus in the electrical picture of Hodgkin and Huxley, there should always be heat dissipation, and the dissipation of heat during the pulse is much larger than the pulse energy. If a nerve had 1 meter of length, the dissipated heat over the whole length would be about 500 times larger than the capacitive energy of the pulse that is the actual signal. Thus the propagation of the nerve pulse in the electrical picture is a very "expensive" process.

12.2 THERMAL AND MECHANICAL PROPERTIES OF NERVE MEMBRANES

Studies on heat release, as considered in the previous section, can in fact be found in the literature. The thermodynamics of the nerve pulse is described next.

12.2.1 Heat Release During the Action Potential

The heat release during action potentials has been measured by a number of authors 4–8. We show some examples from different nerves, both myelinated and nonmyelinated (Figs. 12.3–12.5).

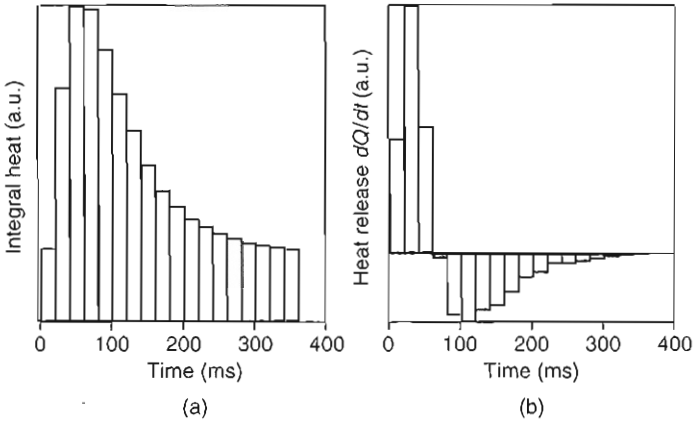

Figure 12.3 (a) Integrated heat and (b) heat release per time during the action potential of nonmyelinated maja nerve bundles (adapted from Ref. 4). A period of heat release is followed by a phase of heat reabsorption. Thus the heat is nearly completely reabsorbed by the nerves, indicating that the physical processes underlying the action potential are mostly reversible processes.

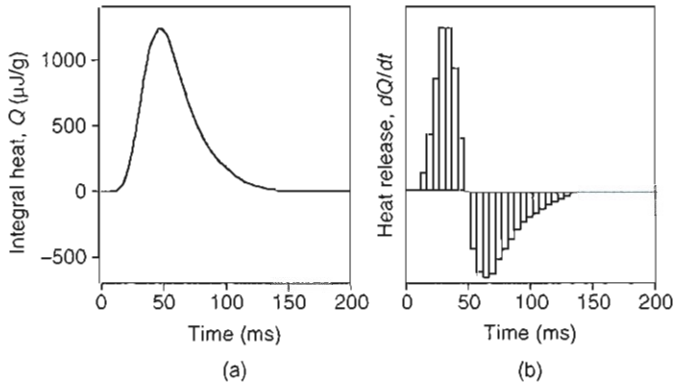

Figure 12.4 Heat production in nonmyelinated fibers of garfish olfactory nerve. (a) The integrated heat (given per gram of nerve) and (b) the differential heat release of the same experiment from a heat block analysis. (Data adapted from Ref. 6.)

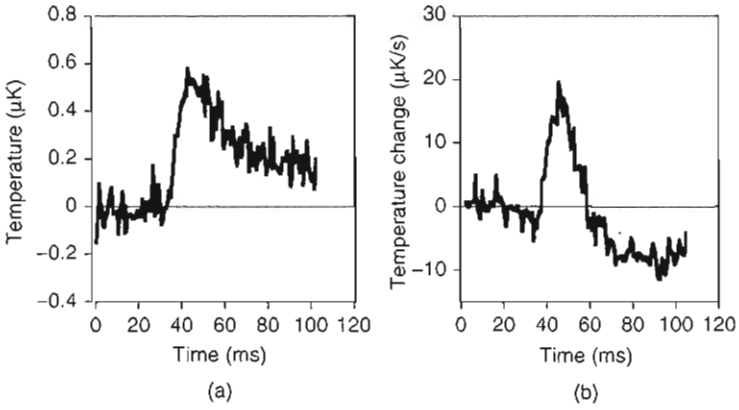

Figure 12.5 Temperature response in myelinated bullfrog sciatic nerve. (a) Absolute temperature change and (b) rate of temperature change indicating the transient release and reabsorption of heat. (Adapted from Ref. 8.)

All authors found the same interesting phenomenon: during the action potential an initial heat liberation is found that is followed by a subsequent heat reabsorption. The total heat of the pulse is zero within experimental error, meaning that the magnitudes of the heat liberation and of the heat absorption are about equal. This is a striking finding that seems to be in conflict with the statements of the Hodgkin–Huxley model that predicts significant positive heat liberation during the nerve pulse due to fluxes of currents (Section 12.4). Interestingly, poisons like tetrodotoxin (that are thought to block ion channels) inhibit the reversible heat pulses [6].

12.2.2 Origin of the Reversible Heat Release

What might be the origin of the reversible heat release? Isn't the presence of a positive and a negative phase of the heat surprising?

The Hodgkin–Huxley picture of the action potential uses equivalent circuits that are an electrical analogy of a biological situation of quite different nature. Instead of electrons flowing along a metal wire, one rather has a flux of hydrated ions through aqueous pores. As already pointed out by Abbott et al. [4], the situation in a nerve resembles much more the expansion of an ideal gas through semipermeable walls. Van't Hoff argued in the 19th century that the concentration of molecules in a solution is closely related to the partial pressure of a gas. Therefore an ion concentration difference across the membrane corresponds to a pressure difference. The concentration of potassium inside the nerve is high (about 400 mM) inside giant squid axons and it is low outside (around 20 mM). For sodium the situation is reversed. According to the Hodgkin–Huxley model, during the action potential the membrane becomes transiently permeable to sodium and potassium. The ions move along their gradients from the high temperature to the low temperature side. During this process, work can be performed by each of the ions. This resembles the motion of a piston during the expansion of an ideal gas. If no work is performed, no heat is absorbed by the system. If work is performed, for instance, by charging the membrane capacitor, heat is absorbed and results in a transient cooling of the nerve. Thus the picture of Hodgkin and Huxley (flux of ions through pores) contains the possibility of cooling even though the electrical analogy is clearly insufficient to describe such effects. Ritchie and Keynes [6] showed that the reversible heat release during the action potential is proportional to the energy of the membrane capacitor given by $E_C = 0.5 C_m U^2$ (Fig. 12.6). They indicated, however, that the reversible heat release is significantly higher than the calculated capacitive energy (see previous section) and thus ruled out that the charging of the capacitor is responsible for the heat changes. For a thorough evaluation of the possible origin of the reversible heat in nerves see Refs. 4 and 5.

In Section 12.1 we showed that the laws of thermodynamics apply to the complete system under consideration but not to arbitrarily separated subsystems. In our present case, the total system is the nerve as a whole, and not just the sum of capacitor, resistors, and other components. Therefore one has to consider the thermal response globally. The fact that the heat changes found in real nerves are within error completely reversible indicates that no net heat is generated and that the entropy of the system remains constant. This is so because $dQ = TdS$ and $\oint dQ/T = 0$, but $\oint dQ = 0$ only holds if one reverses the path when moving back to the original state. This statement must be true for the total nerve even if one can imagine individual processes that release and the absorb heat. If one makes the analogy between the expansion of a gas and the performance of work on the membrane capacitor, a reversible heat change can only be generated by a reversible expansion of a gas. During expansion of the gas the capacitor is charged and heat is absorbed, while discharging of the capacitor compresses the gas, leading to the same concentration differences as before the pulse. This is

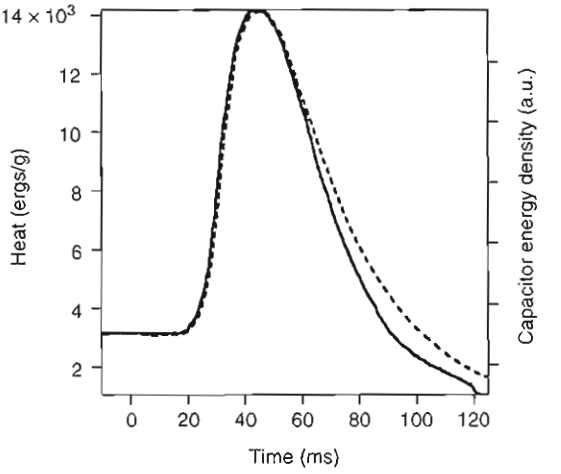

Figure 12.6 Integrated heat release (solid line) and capacitor energy density (dashed line) for garfish olfactory nerve. The two functions are proportional but of different magnitude. (Adapted from Ref. 6.)

definitely not the situation in the Hodgkin–Huxley model in which the pulse generation is driven by permanent fluxes of the ions along their gradients, but never against their gradients.

12.2.3 Mechanical and Structural Changes During the Action Potential

It has been shown by the group of I. Tasaki that the action potential is also accompanied by mechanical and structural changes.

If a thin piston is placed on a squid axon it is displaced by about 1 nm during the nerve pulse (Fig. 12.7b). Simultaneously, a force of up to 2 nN acts on the piston. Both force and dislocation are, within experimental error, proportional to the action potential. Similar results were reported in Refs. 7, 9 and 11–14. These findings indicate that the Hodgkin–Huxley model cannot be complete because it does not contain any mechanical element. If the change in the dimensions of the nerve is due to changes in the membrane thickness, then it is likely that the capacitance is in fact not constant during the action potential. This, however, was assumed by Hodgkin and Huxley [1].

Another interesting finding is that some fluorescence markers alter their fluorescence properties during the action potential [15–19]. In Fig. 12.8 we show the fluorescence changes of the membrane marker pyronine B during the action potential in crab nerves. The fluorescence displays a difference in the two polarization planes. This indicates changes in fluorescence anisotropy and related changes in membrane viscosity during the action potential. For this reason, it has been proposed that the action potential is accompanied by structural changes

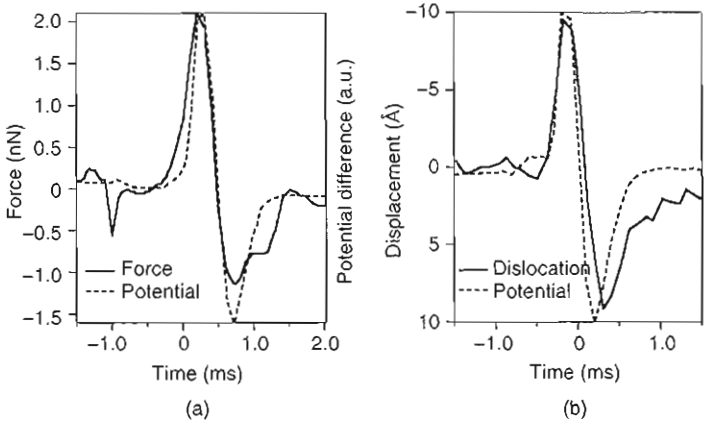

Figure 12.7 Mechanical changes during the action potential. (a) Force on a piston during the action potential in a squid axon. The solid line represents the voltage changes, the dotted curve the force. (b) During the nerve pulse in a squid axon the thickness of the nerve changes proportional to the voltage. (Data adapted from Ref. 10.)

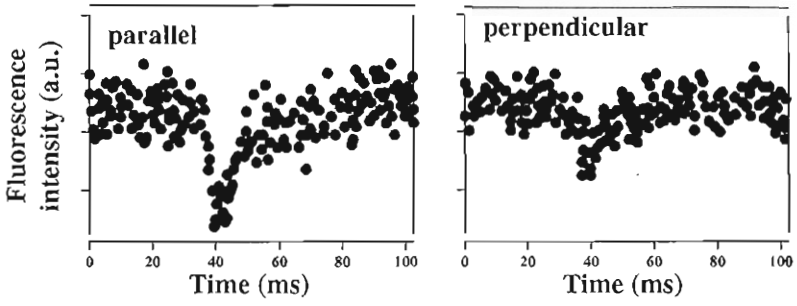

Figure 12.8 Changes of the fluorescence of pyronine B during the action potential of crab nerves (Adapted from Ref. 19). The differences in the fluorescence changes between parallel and perpendicular polarization indicate changes in the rotational anisotropy of the membrane components. This indicates changes in the membrane viscosity. Kobatake et al. [19] concluded from these data that the macromolecules of the nerve membranes undergo structural changes during the action potential.

in the macromolecules and that it is related to transitions in either macromolecules or membranes [14, 19–21].

12.3 PROPAGATING PULSES IN CYLINDRICAL MEMBRANES

The possibility of transitions in the nerve membranes is explored in this section. We show that the thermodynamic findings described earlier can be explained

if one assumes that the action potential consists of propagating density pulses. Heimburg and Jackson [21] demonstrated that one could obtain stable propagating density pulses in cylindrical lipid membranes provided that the membrane exists in a physical state slightly above a melting transition. In the following we outline the underlying basis of this model.

12.3.1 Melting in Biological Membranes and Changes in the Elastic Constants

Many biological membranes display melting transitions slightly below body temperature [3, 21, 22, 39]. It is known that the lipid compositions of bacteria and also of fish cells change as a function of growth temperature and hydrostatic pressure [23–26]. In Fig. 12.9 the melting transitions of native *Escherichia coli* membranes (including all their proteins) are shown. One finds a pronounced lipid melting peak slightly below body temperature that is affected by growth temperature of the bacteria, by hydrostatic pressure, and by pH [3]. Furthermore, one finds several protein unfolding peaks slightly above body temperature. We assume in the following that lipid melting processes slightly below physiological temperature are common and that they exist in nerve membranes.

The melting transitions of such membranes display a melting temperature, T_m, a melting enthalpy, ΔH, and a melting entropy, ΔS, given by $\Delta S = \Delta H / T_m$.

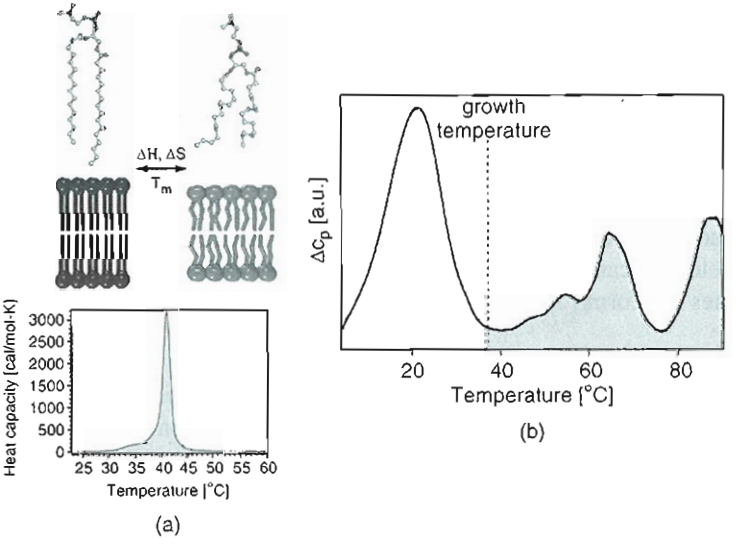

Figure 12.9 (a) Schematic picture of the melting process in lipid membranes and the associated change in the specific heat capacity. (b) Melting profile of the native membranes of *E. coli* grown at 37 °C. The growth temperature is indicated as a dashed line. The peaks below growth temperature belong to the melting of lipid membranes; the peaks shaded in grey above the growth temperature are attributed to protein unfolding. (From Ref. 3.)

Furthermore, volume and area of the membrane change during the melting process. For the model lipid DPPC (dipalmitoyl phosphatidylcholine), a major lipid component of lung surfactant, one finds $T_m = 314.2$ K, $\Delta H = 35$ kJ/mol, $\Delta S = 111.4$ J/mol·K, $\Delta V/V = 0.04$, and $\Delta A/A = 0.246$. These values give the order of magnitude but vary between different lipid species.

The heat capacity, shown for the *E. coli* membranes in Fig. 12.9, is related to the fluctuations in enthalpy through the relation

$$c_P = \frac{\langle H^2 \rangle - \langle H \rangle^2}{RT^2} \tag{12.13}$$

The isothermal and the area compressibility are related to the fluctuations in volume and area as

$$\kappa_T^V = \frac{\langle V^2 \rangle - \langle V \rangle^2}{\langle V \rangle \cdot RT} \quad \text{and} \quad \kappa_T^A = \frac{\langle A^2 \rangle - \langle A \rangle^2}{\langle A \rangle \cdot RT} \tag{12.14}$$

It has been shown [27, 28] that in the chain melting transition volume and area changes are proportional to enthalpy changes. Therefore, in the lipid melting transition, the heat capacity is directly related to the excess isothermal volume and area compressibility, such that one obtains the following relation for the area compressibility:

$$\kappa_T^A(T) = \kappa_{T,0}^A(T) + \Delta\kappa_T^A(T) = \kappa_{T,0}^A(T) + \frac{\gamma_A^2 T}{A} \Delta c_P(T) \tag{12.15}$$

The function $\kappa_{T,0}^A$ is the temperature-dependent area compressibility of the pure phases, which has to be taken from the literature. The factor γ_A assumes the values $\gamma_A = 0.89$ m^2/J. One can see that the area compressibility assumes a maximum at the temperature where the heat capacity is at maximum.

The adiabatic compressibility, important for the determination of the lateral sound velocity, can be determined once the isothermal compressibility is known. It assumes the form [27]

$$\kappa_S^A = \kappa_T^A - \frac{T}{A \cdot c_P} \left(\frac{dA}{dT} \right)_\Pi^2 \tag{12.16}$$

where the heat capacity c_P is that of the membrane plus the aqueous environment that transiently absorbs heat from the membrane upon compression. For a periodic density variation, it is therefore a function of frequency (for details see Ref. 27). It is obviously smaller than the isothermal compressibility. Therefore one concludes that the adiabatic compressibility is in general frequency dependent, meaning that dispersion is found. The frequency dependence of relaxation phenomena in the lipid melting transition has also been documented in experiments [29, 30]. While moving a membrane through the lipid melting transition, the lateral density, ρ^A, of the membrane decreases and the specific area, A, increases. It has been shown

by Heimburg [27] that the change in membrane area, ΔA, is proportional to the change in enthalpy. The heat capacity is defined by $c_P = (dH/dT)_P$. Thus the lateral compressibility becomes a nonlinear function of density that can be calculated from experimental heat capacity data.

The lateral sound velocity within the membrane plane is given by

$$c = \sqrt{\frac{1}{\kappa_S^A \rho^A}} \tag{12.17}$$

The adiabatic compressibility is a nonlinear function of the area density of the membrane, and it follows that the sound velocity is a nonlinear function of the density that close to the lipid melting transition can be expanded into a power series, such that

$$c^2 = c_0^2 + p(\Delta\rho^A) + q(\Delta\rho^A)^2 + \cdots \tag{12.18}$$

where c_0 is the sound velocity in the fluid phase of the membrane. p and q are parameters that have to be determined from the known dependence of the sound velocity on the density. For unilamellar DPPC membranes slightly above the transition, one finds experimentally that $c_0 = 176.6$ m/s (the lateral sound velocity in the fluid phase at low frequencies), $p = -16.6c_0^2/\rho_0^A$, and $q = 79.5c_0^2/(\rho_0^A)^2$ (for details see Ref. 21). Here, $\rho_0^A = 4.035 \times 10^{-3}$ g/m^2 is the lateral area density in the fluid phase of the membrane slightly above the melting point. Similar values were found for lung surfactant or native *E. coli* membranes.

12.3.2 Mechanical Pulses

In the following we explore propagation phenomena in cylindrical membranes. It has been shown by Heimburg and Jackson [21] that the propagation of density changes can be described by the following hydrodynamic relation:

$$\frac{\partial^2}{\partial t^2}\Delta\rho^A = \frac{\partial}{\partial x}\left[c^2\frac{\partial}{\partial x}\Delta\rho^A\right] - h\frac{\partial^4}{\partial x^4}\Delta\rho^A \tag{12.19}$$

The second term is chosen ad hoc to describe the frequency dependence of the sound velocity in a linear way using a parameter h (for details see Ref. 21). It implies that the frequency dependence of the sound velocity is linearly related to the frequency, which is just a first-order approximation. Nerve pulses typically last several milliseconds. Therefore the frequency regime of interest is the kilohertz regime. Unfortunately, the frequency dependence of lipid membranes in the melting transition has not been investigated in this range. In other frequency regimes, however, the frequency dependence of the sound velocity is well known [29, 30]. The parameter h is the only one that has not yet been determined in an experiment. We will see later that the only role of the parameter h is to set the linear scale of the propagating pulse.

We have shown earlier that the sound velocity is a function of the area density, ρ^A. Introducing Eq. (12.18) into Eq. (12.19), we obtain

$$\frac{\partial^2}{\partial t^2}\Delta\rho^A = \frac{\partial}{\partial x}\left[(c_0^2 + p\Delta\rho^A + q(\Delta\rho^A)^2 + \cdots)\frac{\partial}{\partial x}\Delta\rho^A\right] - h\frac{\partial^4}{\partial x^4}\Delta\rho^A \quad (12.20)$$

and after the coordinate transformation $z = x - v \cdot t$ (introducing the propagation velocity, v) we arrive at the time-independent form describing the shape of a propagating density excitation:

$$v^2\frac{\partial^2}{\partial z^2}\Delta\rho^A = \frac{\partial}{\partial z}\left[(c_0^2 + p\Delta\rho^A + q(\Delta\rho^A)^2 + \cdots)\frac{\partial}{\partial z}\Delta\rho^A\right] - h\frac{\partial^4}{\partial z^4}\Delta\rho^A \quad (12.21)$$

This equation has an analytical localized solution [31]:

$$\Delta\rho^A(z) = \frac{p}{q}\cdot\frac{1 - \left(\dfrac{v^2 - v_{\min}^2}{c_0^2 - v_{\min}^2}\right)}{1 + \left(1 + 2\sqrt{\dfrac{v^2 - v_{\min}^2}{c_0^2 - v_{\min}^2}}\cosh\left(\dfrac{c_0}{h}z\sqrt{1 - \dfrac{v^2}{c_0^2}}\right)\right)} \quad (12.22)$$

Such localized solutions are known as solitary waves or solitons. Here we see that the linear scale is proportional to z/h. Therefore the only influence of the parameter h on the solution of the differential equation in Eq. (12.21) is to introduce a scaling factor for the pulse length. A representative soliton profile is shown in Fig. 12.10. The minimum velocity $v_{\min}$ in Eq. (12.22) is given by

$$v_{\min} = \sqrt{c_0^2 - p^2/6q} \quad (12.23)$$

$v_{\min}$ of a soliton in DPPC membranes is found to be $v_{\min} = 115$ m/s, which is very close to the velocity of the action potential found in myelinated nerves. The minimum velocity is the velocity of the soliton when its amplitude reaches the maximum value

$$\Delta\rho_{\max}^A = |p|/q \quad (12.24)$$

corresponding to an overall density change of $\Delta\rho_{\max}^A/\rho_0^A = 0.21$ (Fig. 12.10). Solitons with larger density change do not exist.

The total area change when going through a melting transition is $\Delta\rho_{\max}^A/\rho_0^A = 0.246$ (for DPPC). Thus at maximum amplitude, the soliton forces the lipid membrane by about 85% through the melting transition. This will cause a transient heat release corresponding to 85% of the melting enthalpy (which is on the order of 35 kJ/mol or ~13 kT per lipid).

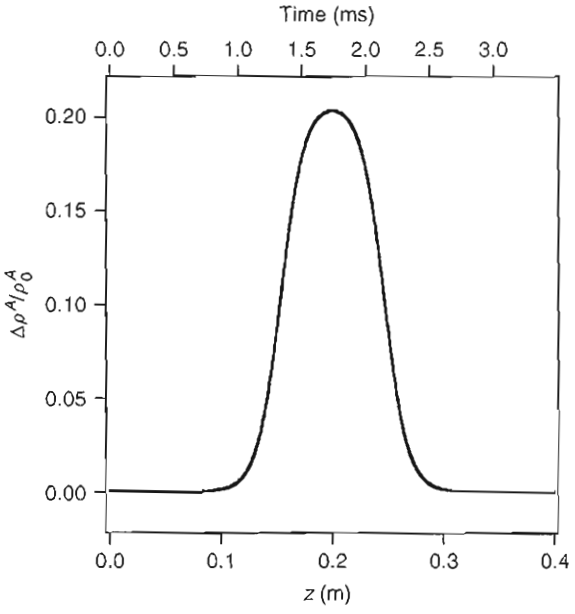

Figure 12.10 Soliton profile for a soliton velocity of $v = 0.651c_0$ calculated for $h = 2\text{m}^4/\text{s}^2$. This soliton has a maximum amplitude of $\Delta\rho^A/\rho_0^A = 0.21$. Its width is approximately 10 cm and it lasts about 1 ms.

During the pulse the membrane is reversibly moved by about 85% through the melting transition. Simultaneously, the thickness of the membrane will change by 85% of the thickness change in the transition from fluid to gel (7.4 Å for DPPC). Since the soliton is linked to changes in lipid state, the fluorescence anisotropy will also change in an experiment. It is well known that the anisotropy (related to the rotational mobility) is higher in the gel phase than in the fluid phase. Such changes have all been found in real nerves under the influence of the action potential (see Section 12.2.3 and reference therein). The order of magnitude of these changes matches the data found for such nerves.

The heat of melting of DPPC is about 35 kJ/mol or 48 J/g of lipid. If the membrane is pushed by 85% through the transition, this corresponds to 40 J/g of lipid. This heat is two orders of magnitude higher than that hypothetically dissipated by the ion currents during a pulse (0.4 J/g, see Section 12.1.3) and more than three orders of magnitude higher than the energy of the membrane capacitor during the action potential (0.01 J/g, see Section 12.1.3). It has been pointed out by Abbott et al. [4] that the positive and negative phases of heat liberation during a pulse are so close in time that in real experiments they are partially averaged out due to the response time of the heat sensor and by its physical size. Therefore the experimentally observed heat is just a low-end estimate of the real heat that must be significantly larger.

The mechanical energy of the solitons can also be calculated by using Lagrangian formalism [21]. The result is that the combined kinetic and potential energy of the soliton is about 40 times larger than the capacitor energy. The heat in the soliton, however, seems to be about 100 times larger than the mechanical energy of the pulse. This is possible close to transitions where the work to compress the membranes is small, and where entropy and internal energy (or enthalpy) changes compensate. This effect is often called entropy–enthalpy compensation. It seems as if the potential energy obtained by Lagrangian formalism is in fact a free-energy change. In transitions, free-energy changes can be very small even if the associated heat and enthalpy changes are large.

12.4 EXCITATION OF THE NERVE PULSE

12.4.1 Pulse Generation

How are the density pulses initiated? As mentioned earlier, the membrane is pushed by 85% through its phase transition during the soliton. Therefore everything that is able to move a lipid membrane through its transition should display the potential to start a pulse. The nature of the solitons that are the solutions to Eq. (12.21) has carefully been investigated [31]. It was found that if one locally generates a gel-like membrane region (domain) in a membrane above the melting transition regime, it should fall apart into two solitons propagating in opposite directions. One possibility to generate local gel domains is a local sudden lowering of temperature. It has been described by Kobatake et al. [19] that in fact nerves start firing when they are cooled locally; while firing is inhibited upon heating. Another possibility to shift membranes through transitions is the local lowering of pH [32]. Biological lipid membranes are typically negatively charged. Lowering of pH leads to protonation of the negatively charged groups. Simultaneously, the melting points of charged membranes increase by up to 20 K. Thus protons may induce a transition in membranes. It is known that action potentials can be triggered by local acidification, but the mechanism is so far not understood [33]. Furthermore, a pulse may be induced by local increase in calcium concentration because it is known that membrane melting transitions shift to higher temperatures upon calcium binding. An increase of calcium concentration from 1.8 to 20 mM has been shown to increase the capability of neuroblastoma cells to fire repetitively [34]. Another possibility to generate pulses is a change in membrane potential due to the electrostatic potential of a negatively charged lipid membrane. This is the most common way to evoke action potentials.

12.4.2 Free Energy of a Pulse

The free energy required to generate a local gel domain is closely related to the distance from the transition midpoint to physiological temperature [35]. At

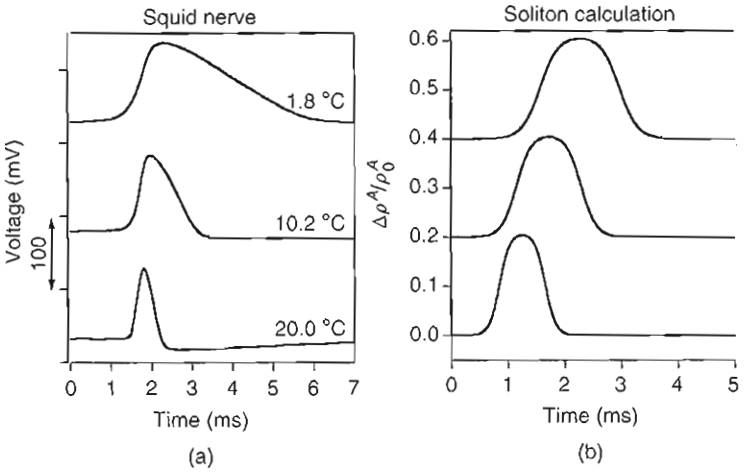

Figure 12.11 Width of the action potential after constant trigger as a function of temperature. (a) Squid action potentials recorded at different temperatures (adapted from Ref. 36). (b) Solitons generated with the same amount of free energy at increasing ambient temperature. As in the squid experiment, the broader signals stem from lower temperatures.

constant pressure it is given by

$$\Delta G = \Delta H \cdot \left(\frac{T_m - T}{T_m} \right) \tag{12.25}$$

If a constant amount of free energy is provided to a nerve (e.g., by a local change in voltage or a fixed number of protons or calcium ions), the pulse will possess smaller energy content when the temperature is higher (because more free energy is required to start the pulse at higher temperatures). This is shown in Fig. 12.11. The solitons display a smaller width when the energy content is smaller. Eventually, the amplitude will also decrease. In experiments on squid axons, it has been found that the width of the action potential becomes smaller when temperature is raised [36].

It has been shown recently [35] that the effect of general anesthetics is also related to the free-energy change necessary to move a membrane through a transition. Anesthetics are known to lower lipid membrane melting points, and thus increase the amount of free energy to start a pulse. This picture is able to quantitatively explain anesthesia. Thus the soliton model automatically implies a mechanism for anesthesia [3, 35].

12.5 CONCLUSION

Thermodynamics is a theory that can be applied to complex systems even if the molecular details of this system are unknown. The second law states that in

equilibrium the entropy assumes a maximum. We have shown that during the action potential of nerves no net heat is dissipated. A phase of heat release is immediately followed by a phase of heat reabsorption. The finding of zero net heat exchange implies a conservation of the entropy of the system (no entropy is dissipated). This means that the entropy after completion of the action potential is the same as before the action potential. The consequence is that the physical processes underlying the action potential must be of reversible nature. The Hodgkin–Huxley model, which is the textbook picture of the nervous impulse, however, is exclusively based on irreversible processes (consisting of fluxes of ions through ion channels from the side of high concentration to that of low concentration) in which entropy is not maintained. The model can therefore not be correct. It may be possible to think about processes that release heat and other processes that absorb heat. Nevertheless, thermodynamics applies to the system as a whole and not to individual subsystems. Therefore the fact that no entropy is dissipated during the nerve pulse has to be taken seriously. It will be impossible to divide the total nerve signal into subprocesses (with some of them releasing and others absorbing heat) that result in an overall heat dissipation of zero and still be consistent with a model based on dissipative processes. For this reason, we described here an alternative approach that assumes that the nervous impulse is an entropic pulse (with zero entropy change after completion of the pulse). Such a pulse would show some features that have been described for nerves: reversible heat release, reversible changes in thickness, and reversible changes in membrane state. Since proteins are parts of biological membranes, they may also contribute to these changes as long as the processes are reversible. A reversible pulse involving proteins is favored by Tasaki [14].

The thermodynamic behavior of artificial and biological membranes gives rise to a number of interesting mechanical features. In particular, slightly below physiological temperature, one finds a cooperative lipid melting transition in which the heat capacity and also the elastic constants assume maxima. Under these conditions, localized mechanical (entropic) pulses called solitons can propagate with a velocity of about 100 m/s, close to that of myelinated nerves. One many loosely refer to them as sound pulses. However, like all mechanical changes, they are linked to changes in other variables of the system including changes in charge density, in the electrostatic potential, in heat content, in nerve thickness, and in lipid chain order parameter. Such changes have been found in real nerves. The classical studies on nerves have focused mainly on measuring voltage changes since they are large (100 mV) and therefore easy to measure. However, many other features change simultaneously and have to be measured to obtain a complete picture of the underlying physical processes. This implies thickness changes, density changes, and heat release, but also transient pH or calcium concentration changes. Thermodynamics clearly helps to reinterpret classical findings on nerve pulse propagation and provide a different viewpoint on processes that are seemingly in conflict with each other.

ACKNOWLEDGMENTS

Thanks to Benny Lautrup at the Niels Bohr Institute, who accompanied the development of these thoughts with major contributions, encouragement, and criticism. We are very grateful to Konrad Kaufmann, who discussed these issues with one of us for many years. Some of these issues have already been pointed out in his earlier manuscripts [37, 38]. We thank Dr. I. Tasaki for his interest and important comments and suggestions.

REFERENCES

1. A. L. Hodgkin and A. F. Huxley (1952). A quantitative description of membrane current and its application to conduction and excitation in nerve. *J. Physiol. (London)* **117**: 500–544.
2. P. L. Privalov (1990). Cold denaturation of proteins. *Crit. Rev. Biochem. Mol. Biol.* **25**: 281–305.
3. T. Heimburg and A. D. Jackson (2007). On the action potential as a propagating density pulse and the role of anesthetics. *Biophys. Rev. Lett.* **2**: 57–78.
4. B. C. Abbott, A. V. Hill, and J. V. Howarth (1958). The positive and negative heat associated with a nerve pulse. *Proc. R. Soc. London B* **148**: 149–187.
5. J. V. Howarth, R. D. Keynes, and J. M. Ritchie (1968). The origin of the initial heat associated with a single impulse in mammalian non-myelinated nerve fibres. *J. Physiol.* **194**: 745–793.
6. J. M. Ritchie and R. D. Keynes (1985). The production and absorption of heat associated with electrical activity in nerve and electric organ. *Q. Rev. Biophys.* **392**: 451–476.
7. I. Tasaki, K. Kusano, and M. Byrne (1989). Rapid mechanical and thermal changes in the garfish olfactory nerve associated with a propagated impulse. *Biophys. J.* **55**: 1033–1040.
8. I. Tasaki and P. M. Byrne (1992). Heat production associated with a propagated impulse in bullfrog myelinated nerve fibers. *Jpn. J. Physiol.* **42**: 805–813.
9. K. Iwasa and I. Tasaki (1980). Mechanical changes in squid giant-axons associated with production of action potentials. *Biochem. Biophys. Res. Commun.* **95**: 1328–1331.
10. K. Iwasa, I. Tasaki, and R. C. Gibbons (1980). Swelling of nerve fibers associated with action potentials. *Science* **210**: 338–339.
11. I. Tasaki, K. Iwasa, and R. C. Gibbons (1980). Mechanical changes in crab nerve fibers during action potentials. *Jpn. J. Physiol.* **30**: 897–905.
12. I. Tasaki and K. Iwasa (1982). Further studies of rapid mechanical changes in squid giant axon associated with action potential production. *Jpn. J. Physiol.* **32**: 505–518.
13. I. Tasaki and M. Byrne (1990). Volume expansion of nonmyelinated nerve fibers during impulse conduction. *Biophys. J.* **57**: 633–635.
14. I. Tasaki (1999). Evidence for phase transition in nerve fibers, cells and synapses. *Ferroelectrics* **220**: 305–316.

15. I. Tasaki, A. Watanabe, R. Sandlin, and L. Carnay (1968). Changes in fluorescence, turbidity, and birefringence associated with nerve excitation. *Proc. Natl. Acad. Sci. USA* **61**: 883–888.

16. I. Tasaki, L. Carnay, and A. Watanabe (1969). Transient changes in extrinsic fluorescence of nerve produced by electric stimulation. *Proc. Natl. Acad. Sci. USA* **64**: 1362–1368.

17. I. Tasaki, L. Carnay, R. Sandlin, and A. Watanabe (1969). Fluorescence changes during conduction in nerves stained with Acridine Orange. *Science* **163**: 683–685.

18. F. Conti and I. Tasaki (1970). Changes in extrinsic fluorescence in squid axons during voltage-clamp. *Science* **169**: 1322–1324.

19. Y. Kobatake, I. Tasaki, and A. Watanabe (1971). Phase transition in membrane with reference to nerve excitation. *Adv. Biophys.* **2**: 1–31.

20. P. K. J. Kinnunen and J. A. Virtanen (1986). A qualitative, molecular model of the nerve pulse. Conductive properties of unsaturated lyotropic liquid crystals, in *Modern Bioelectrochemistry* (F. Gutmann and H. Keyzer, Eds.). Plenum Press, New York, pp. 457–479.

21. T. Heimburg and A. D. Jackson (2005). On soliton propagation in biomembranes and nerves. *Proc. Natl. Acad. Sci. USA* **102**: 9790–9795.

22. J. L. C. M. van de Vossenberg, A. J. M. Driessen, M. S. da Costa, and W. N. Konings (1999). Homeostasis of the membrane proton permeability in *Bacillus subtilis* grown at different temperatures. *Biochim. Biophys. Acta* **1419**: 97–104.

23. S. V. Avery, D. Lloyd, and J. L. Harwood (1995). Temperature-dependent changes in plasma membrane lipid order and the phagocytic activity of the *Amoeba acanthamoeba castellanii* are closely correlated. *Biochem. J.* **312**: 811–816.

24. E. F. DeLong and A. A. Yayanos (1985). Adaptation of the membrane lipids of a deep-sea bacterium to changes in hydrostatic pressure. *Science* **228**: 1101–1103.

25. J. R. Hazel (1979). Influence of thermal acclimation on membrane lipid composition of rainbow trout liver. *Am. J. Physiol. Regul. Integrative Comp.Physiol.* **287**: R633–R641.

26. J. R. Hazel (1995). Thermal adaptation in biological membranes: Is homeoviscous adaptation the explanation? *Annu. Rev. Physiol.* **57**: 19–42.

27. T. Heimburg (1998). Mechanical aspects of membrane thermodynamics. Estimation of the mechanical properties of lipid membranes close to the chain melting transition from calorimetry. *Biochim. Biophys. Acta* **1415**: 147–162.

28. H. Ebel, P. Grabitz, and T. Heimburg (2001). Enthalpy and volume changes in lipid membranes. I. The proportionality of heat and volume changes in the lipid melting transition and its implication for the elastic constants. *J. Phys. Chem. B* **105**: 7353–7360.

29. S. Mitaku and T. Date (1982). Anomalies of nanosecond ultrasonic relaxation in the lipid bilayer transition. *Biochim. Biophys. Acta* **688**: 411–421.

30. S. Halstenberg, W. Schrader, P. Das, J. K. Bhattacharjee, and U. Kaatze (2003). Critical fluctuations in the domain structure of lipid membranes. *J. Chem. Phys.* **118**: 5683–5691.

31. B. Lautrup, A. D. Jackson, and T. Heimburg (2005). The stability of solitons in biomembranes and nerves. (http://www.arXiv.org/biophysics/0510106).

32. H. Träuble, M. Teubner, P. Woolley, and H. Eibl (1976). Electrostatic interactions at charged lipid membranes. 1. Effects of pH and univalent cations on membrane structure. *Biophys. Chem.* **148**: 319–342.

33. M. Vukicevic and S. Kellenberger (2004). Modulatory effects of acid-sensing ion channels on action potential generation in hippocampal neurons. *Am. J. Physiol. Cell Physiol.* **287**: C682–C690.

34. W. H. Moolenaar and I. Spector (1979). The calcium action potential and a prolonged calcium dependent after-hyperpolarization in mouse neuroblastoma cells. *J. Physiol.* **292**: 297–306.

35. T. Heimburg and A. D. Jackson (2007). The thermodynamics of general anesthesia. *Biophys. J.* **92**: 3159–3165.

36. J. J. C. Rosenthal and F. Bezanilla (2000). Seasonal variation in conduction velocity of action potentials in squid giant axons. *Biol. Bull.* **199**: 135–143.

37. K. Kaufmann (1989). Action potential, Caruaru (http://membranes.nbi.dk/Kaufmann/pdf/Kaufmann_book4_org.pdf).

38. K. Kaufmann (1989). Lipid membrane Caruaru (http://membranes.nbi.dk/Kaufmann/pdf/Kaufmann_book5_org.pdf).

39. M. Larsson, T. Nylander, K. M. W. Keough, and K. Nag (2006). An X-ray diffraction study of alterations in bovine lung surfactant bilayer structures induced by albumin. *Chem. Phys. Lipids* **144**: 137–145.